Deep Distributed Learning-based POI Recommendation Under Mobile Edge Networks

Zhiwei Guo, *Member, IEEE,* Keping Yu, *Member, IEEE,* Neeraj Kumar, *Senior Member, IEEE,* Wei Wei, *Senior Member, IEEE,* Shahid Mumtaz, *Senior Member, IEEE* and Mohsen Guizani, *Fellow, IEEE*

***Abstract*—With the rapid development of edge intelligence in wireless communication networks, mobile edge networks (MEN) have been broadly discussed in academia. Supported by considerable geographical data acquisition ability of mobile Internet of Things (IoT), the MEN can also provide spatial locations-based social service to users. Therefore, suggesting reasonable points-of-interest (POIs) to users is essential to improve user experience of MEN. As the simple user-location data is usually sparse and not informative, existing literature attempted to extend feature space from two perspectives: contextual patterns and semantic patterns. However, previous approaches mainly focused on internal features of users, yet ignoring latent external features among them. To address this challenge, in this paper, a deep distributed learning-based POI recommendation (Deep-PR) method is proposed for situations of MEN. In particular, hidden feature components from both local and global subspaces are deeply abstracted via representative learning schemes. Besides, propagation operations are embedded to iteratively reoptimize expressions of the feature space. The successive effect of the above two aspects contributes a lot to more fine-grained feature spaces, so that recommendation accuracy can be ensured. Two types of experiments are also carried out on three real-world datasets to assess both efficiency and stability of the proposed Deep-PR. Compared with seven typical baselines with respect to four evaluation metrics, obtained results of the overall performance of the Deep-PR are excellent.**

This work was supported in part by the National Natural Science Foundation of China under grant 62106029, in part by the Humanities and social Science Research Project of the Ministry of Education under grant 21YJC630036, in part by the Science and Technology Research Program of Chongqing Municipal Education Commission under Grant KJQN202000805, in part by key program of CTBU under grant KFJJ2018060 and grant 1856033, in part by the Japan Society for the Promotion of Science (JSPS) Grants-in-Aid for Scientific Research (KAKENHI) under Grant JP18K18044 and JP21K17736.

(*Corresponding author: Keping Yu*)

Zhiwei Guo is with Chongqing Key Laboratory of Intelligent Perception and BlockChain Technology, National Research Base of Intelligent Manufacturing Service, Chongqing Technology and Business University, Chongqing 400067, China (e-mail: zwguo@ctbu.edu.cn).

Keping Yu is with School of Computer and Information Engineering, Bengbu University, Bengbu 233000, China, also with Graduate School of Science and Engineering, Hosei University, Tokyo 184-8584, Japan, and also with RIKEN Center for Advanced Intelligence Project, RIKEN, Tokyo 103-0027, Japan (e-mail: keping.yu@ieee.org).

Neeraj Kumar is with the Department of Computer Science and Engineering, Thapar Institute of Engineering, India, also with School of Computer Science, University of Petroleum and Energy Studies, Dehradun, Uttarakhand, India, also with Department of Computer Science and Information Engineering, Asia University, Taiwan, and also with King Abdul Aziz University, Jeddah, Saudi Arabia. (e-mail: neeraj.kumar@thapar.edu).

Wei Wei is with School of Computer Science and Engineering, Xi'an University of Technology, Xi'an 710048, China (email: weiwei@xaut.edu.cn).

Shahid Mumtaz is with Nottingham Trent University, Uk (e-mail: Dr.shahid.mumtaz@ieee.org).

Mohsen Guizani is with the Machine Learning Department, Mohamed Bin Zayed University of Artificial Intelligence (MBZUAI), UAE (e-mail:mguizani@ieee.org).

***Index Terms*—Deep distributed learning, mobile edge networks, point-of-interest, deep information fusion.**

I. INTRODUCTION

THE rapid development of novel communication technologies such as mobile Internet of Things (IoT) has brought profound changes to human society [1]. On the basis of proper ability of mobile data integration and management, mobile IoT provide a resilient information sharing medium for people [2]. Supported by efficient mobile IoT environment, users of mobile computing can obtain convenient location-based social services anytime and everywhere. At the same time, the continuous increase of mobile access also produces growing amount of data transmission [3]. This not only brings serious workload to wireless infrastructures, but also affects the privacy security of users to a great extent [4]. In this context, mobile edge computing under support of mobile IoT has been regarded as a promising solution to this problem [5]. It uses nearest computation nodes in wireless networks to provide computing service for users, in order to create service environment with high performance, low latency and high bandwidth [6]. It can be predicted that mobile edge networks (MEN) will become important support for 5g communication networks in the future [7]. Accordingly, it is of great significance to provide efficient personalized services for users of MEN [8].

The most typical service in MEN is location-based recommendation which has been a hot concern in in general mobile networks (GMN) [9]. Because users always cannot discover feasible points-of-interest (POIs) which refer to places they are interested in [10]. The analysis towards user-location data, however, is still confronted with two aspects of challenges [11]. For one thing, simple user-location data are not informative, and cannot reveal comprehensive preference characteristics [12]. It is expected to fuse associated multi-source information to realize distributed learning. For another, user-location data is usually sparse for it is not easy to be acquired [13]. It is supposed to enrich sample spaces by reasonably mining internal associations. As MEN distributes computational power into a number of edge nodes, these challenges are even obvious.

In recent years, researchers have dealt with these difficulties by leveraging two types of features: contextual patterns [14]-[24] and semantic patterns [25]-[34]. The former refers to inherent characteristics of users, e.g., preferences, social relations, activity records, while the latter refers to textual contents associated with locations, such as reviews and tags.

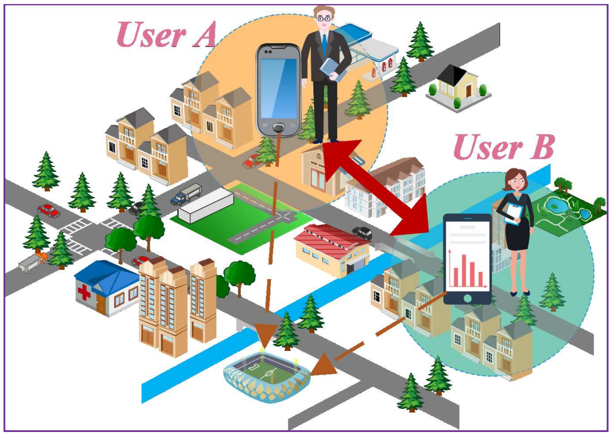

Fig. 1: A typical example to illustrate potential correlations among users.

Nevertheless, almost all of previous research view each user as a unique object, and focus on visible explicit features inside them. Thus, imperceptible external features such as latent relevance among users are universally neglected. In fact, implicit linkages among different users exist to some extent, and are helpful to enrichment of feature spaces. And the Fig. 1 is developed here as a typical example of MEN to illustrate such view. User A and User B have their own daily wandering areas, respectively corresponding to two circles in different colors. Naturally, edge computing services received by them are related to nodes close to their activity circles, respectively. It is assumed that they are both teachers and have correlations in works. Such point is not explicit, and cannot be directly indicated by contextual or semantic features. Therefore, the perspective of distributed learning is required to be introduced to learn comprehensive feature spaces, so that POI recommendation efficiency in MEN can be promoted. To facilitate this, deeper-level and more abstract feature expressions need to be extracted to enhance properly depth of feature space.

As consequence, feature space of a user is categorized into local subspace and global subspace. The local part emphasizes inherent features of the user himself, and the global part focuses on external latent relevance. The two subspaces are respectively reoptimized through propagation operations. Thus in this paper, a **Deep** distributed learning-based **P**OI **R**ecommendation (Deep-PR) model is proposed for MEN applications. Specifically, a hybrid adaptive encoder (HAE) and a correlated adaptive encoder (CAE) are developed for deep-level encoding of local features and global features, respectively. Both of the two encoders end with propagation operations, aiming to reoptimize feature space to enhance its representative ability. After that, two real-world datasets are selected as experimental scenarios, and three groups of experiments are conducted to evaluate overall performance of the proposed Deep-PR. Experimental results on three real-world datasets show that the Deep-PR outperforms baselines in terms of precision and stability. To the best of our knowledge, no research had deeply extracted both internal and external features to improve POI recommendations. It is believed that better POI recommendation effect is able to inversely promote healthy development of mobile IoT as well as the MEN.

The rest of this paper is organized as follows. Firstly, general situation of the research problem is explained in Section II. In Section III, mathematical descriptions of technology method are given in detail. Then, Section IV demonstrates empirical experiments that evaluate performance of the Deep-PR. Finally, Section V concludes this paper.

II. Preliminaries

A. Problem Statement

As location data is a two-dimensional vector with two precise values of longitude and latitude, close locations always have different coordinate values. Instead, concept of POI is defined as follows:

Definition 1 (POI): The whole geographical space is separated into a number of block cells with roughly equal area. Each separated cell is defined as a POI, and all the initial location data is transformed into corresponding POIs.

Let $u_i \, (i = 1, 2, \cdots, |u|)$ denote the set of $|u|$ users, and $p_j \, (j = 1, 2, \cdots, |p|)$ denote the set of $|p|$ POIs. Each user is allowed to interact with any POI once or multiple times. For user u_i, he never has direct preference feedback towards POIs. Thus, the interaction value q_{ij} can be viewed as indirect preference feedback. The generation of interaction value between user u_i and POI p_j is mainly determined by both local features and global features which are defined as:

Definition 2 (Local Features): Local features are defined as characteristics existing inside entities: contextual features of users and semantic features of positions.

Definition 3 (Global Features): Global features are defined as latent linkages among users of the whole feature space: static relevance and dynamic relevance.

Due to the general data sparsity of such type of scenes, deep representation is introduced to construct a more fine-grained feature space. To begin with, the Deep-PR is established upon the basis of following assumptions:

Assumption 1: Each user is associated with information of social relations.

Assumption 2: Each POI is associated with some textual contents which may come from reviews, tags or descriptions.

Assumption 3: Interaction records of users are associated with time information, so that they can be ranked sequentially.

B. Related Work

As the people are more and more concerned in service quality of LBSN, POI recommendation techniques have already been a key research topic for many LBSN operators. The macroscopic POI recommendation problem is able to yield more than one branches. Some researchers consider single geography features of POIs, some add contextual features of POIs into consideration, and some further consider preference characteristics of users in LBSN. Of all the various research works, technical methods include statistical learning, machine learning, deep learning, etc. Some typical works are surveyed in this part.

Liu et al. [38] managed to generate more robust feature representation format for users inside check-in records. In

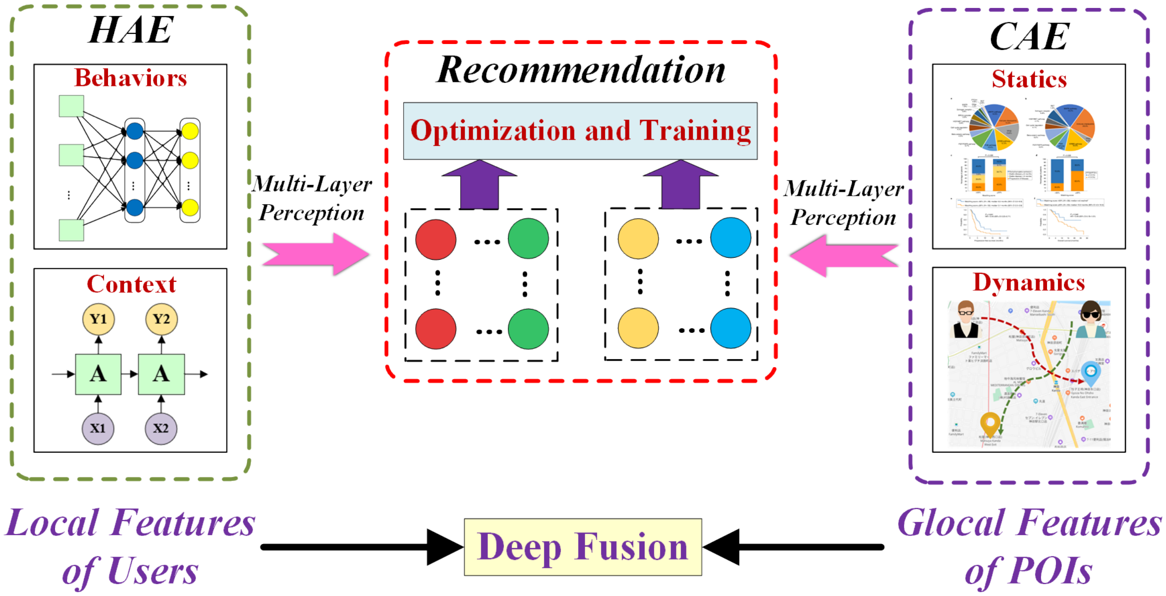

Fig. 2: Workflow of the proposed Deep-PR.

terms of user preference, the relative pair-wise preference ranking is introduced to represent it.

Yu et al. [39] incorporated user preference and context information of POIs to propose a context- and preference-aware model which is named as CPAM for short. It is composed of two parts: POI embedding and logistic matrix factorization.

Aliannejadi et al. [33] introduced the collaborative ranking into temporal POI recommendation, and presented a two-stage approach for this purpose. The method considered geographical influence of POIs, and used variance of POIs popularity to construct regularizer.

Wang et al. [16] developed a geography-aware inductive matrix completion model to suggest unknown POIs for users. It utilized Gaussian mixture model to extraction features for POIs, and constructed an inductive matrix completion model for output.

Huang et al. [41] proposed introduced attention mechanism to propose a novel spatiotemporal long short-term memory model which is named as ATST-LSTM for short. It can take both geographical context and influence of POIs into consideration.

It can be deduced from the existing literatures that they were mostly developed under emphasis of some specific aspects. There still lacks a comprehensive framework that can deeply fuse global information for POI recommendation. Therefore, this paper aims at this point and proposes the Deep-PR.

III. Methodology

A. Overview

Fig 2 gives main workflow of the proposed Deep-PR which is actually an architecture of deep information fusion. It is composed of three major parts: HAE part, CAE part, and recommendation part. On the one hand, an HAE is developed to learn a representative vector L_{ij} between user u_i and POI p_j. The dimension of L_{ij} equals to the number of his interaction records. On the other hand, a CAE is developed to learn a representative matrix G_i for user u_i. It denotes relevance between user u_i and every other $(|u|-1)$ users. Having encoded two aspects of features, expressions of generating interaction values can be formulated accordingly. Given known interaction values between users and POIs, the task is to suggest user u_i other POIs he may be interested in.

As is shown in Fig. 2, major novelty of the proposed Deep-PR actually lies in a deep information fusion framework. The HAE part and CAE part implement deep representation operation towards different features, respectively. Macroscopically, the Deep-PR can be viewed as a distributed learning framework between HAE and CAE, contributes a robust and deep-level recommendation system. To this end, main contributions of the proposed Deep-PR approach can be summed up as following aspects:

1) To recommend a more precise POI for users of MEN, the Deep-PR enhances feature spaces by refining both internal and external features.
2) The Deep-PR implements a distributed learning framework, in which two modules carry out deep information fusion operations separately. Such design leads to a deep-level recommendation framework.

B. Modeling of Local Features

Major goal of this subsection is to learn the parametric representative vector L_{ij} between user u_i and POI p_j. Such function is mainly realized by the HAE part. Fig. 3 gives main workflow of the HAE part which is composed by two basic models: convolutional neural network (CNN) and bidirectional attentive network (Bi-AN). The CNN manages to encode contextual patterns of user u_i, and the Bi-AN manages to encode semantic patterns of p_j. The two factors are further fused into the final L_{ij} via a multi-round propagation process.

1) Contextual Features: In this research, contextual features mainly refer to social relations of users. In the CNN part of developed HAE, a combination of convolution operation and pooling operation is viewed as a processing layer. Role of each processing layer is to carry out feature extraction and dimension reduction towards initial features. The number of processing layers is a variable and denoted as M. In other words, initial input features are transformed into a contextual feature vector $R_i^{(Co)}$ via M successive processing layers.

As for user u_i, his social relation vector can be established through binary encoding and is represented as:

$$A_s = \left\{ s_{i,1}, s_{i,2}, \cdots, s_{i,i-1}, s_{i,i+1}, \cdots, s_{i,|u|} \right\} \tag{1}$$

where $s_{i,i-1}$ denotes social status between user u_i and user u_{i-1}. Note that $s_{i,i-1}$ equals to 1 if the social relation exists and equals to 0 otherwise. To construct input matrix for CNN, it is expected to map the vectorized A_s into another $|u-2| \times$ 3-dimensional matrix $A_S^{(1)}$. Each adjacent three elements are selected in turn to construct rows of the $A_S^{(1)}$ whose format is as:

$$A_s^{(1)} = \begin{bmatrix} s_{i,1} & s_{i,2} & s_{i,3} \\ s_{i,2} & s_{i,3} & s_{i,4} \\ \vdots & \vdots & \vdots \\ s_{i,(|u|-2)} & s_{i,(|u|-1)} & s_{i,|u|} \end{bmatrix} \tag{2}$$

As the rank of $A_S^{(1)}$ is only three, it is required to be further transformed into the input feature matrix $A_S^{(2)}$ through the following nonlinear mapping:

$$A_s^{(2)} = \sigma_1 \left\{ W_{L1} \cdot F_1 \left[A_s^{(1)} \right] + b_{L1} \right\} \tag{3}$$

where W_{L1} is weight parameter, b_{L1} is bias parameter, $\sigma_1(x) = \max(0, x)$ denotes the Rectified Linear Unit (ReLU) activation function, and $F_1(\cdot)$ is a non-linear mapping function represented as:

$$F_1 \left[A_s^{(1)} \right] = \frac{1}{\eta} \sum_{\theta=1}^{\eta} \left\{ a_i \cdot \left[A_{s,\theta}^{(1)} \right]^T \right\} \tag{4}$$

where a_i is the attention weight, $A_{s,\theta}^{(1)} (\theta = 1, 2, \cdots, \eta)$ is the enumeration of all elements in $A_s^{(1)}$. The obtained $A_s^{(2)}$ is an $(m-2) \times (m-2)$-dimensional matrix.

In convolution operation of the m-th processing layer, inner product calculation is conducted between $A_s^{(2)}$ and a series of N-core filtering matrices W_n. Among, n is the index number of convolutional cores. Another matrix $A_L^{(m)}$ is obtained via the following nonlinear mapping:

$$A_L^{(m)} = \sigma_1 \left\{ W_L^{(n)} \otimes A_s^{(2)} + b_L^{(n)} \right\} \tag{5}$$

where $\otimes$ denotes convolution operator, and b_{L-n} is the series of N bias parameters. In pooling operation of the m-th processing layer, $A_L^{(m)}$ is further compacted through common max-pooling criteria, leading to another matrix $A_{L-pool}^{(m)}$. It will be transformed via a fully connected computation. The process is expressed as the following formula:

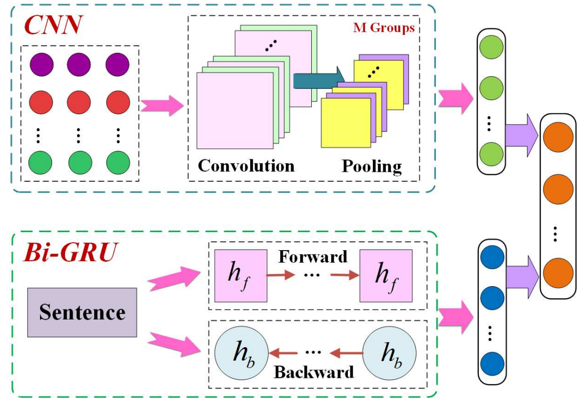

Fig. 3: Illustration of the HAE architecture.

$$R_i^{(Co)} = \sigma_1 \left\{ \sum_{m=1}^{M} \left[W_{L2} \otimes A_{L-pool}^{(m)} + b_{L2} \right] \right\} \tag{6}$$

The obtained $R_i^{(Co)}$ is the feature factor of contextual features.

2) Semantic Features: As for j-th POI, all the textual information is viewed as a sentence including V words. The gated recurrent unit (GRU) network is utilized to model sequential characteristics from both forward and backward directions. Hidden semantic embeddings of two directions are represented as:

$$H_{j,v}^{(f)} = \overrightarrow{GRU} \left[H_{j,(v-1)}^{(f)} \right] \tag{7}$$

$$H_{j,v}^{(b)} = \overleftarrow{GRU} \left[H_{j,(v+1)}^{(b)} \right] \tag{8}$$

where v is the index number of V words in the sentence. The hidden semantic vector is constructed by concatenation of above two objects:

$$H_{j,v} = H_{j,v}^{(f)} \oplus H_{j,v}^{(b)} \tag{9}$$

It will then be mapped into semantic feature vector via the following formula:

$$R_j^{(Se)} = \sigma_1 \left\{ W_{L3} \cdot F_2 \left(H_{j,v} \right) + b_{L3} \right\} \tag{10}$$

where W_{L3} is weight parameter, b_{L3} is bias parameter, and $F_2(\cdot)$ is an attention-based mapping function represented as:

$$F_2 \left(H_{j,v} \right) = \sum_{v=1}^{V} \left[a_j \cdot \left(H_{j,v} \right)^T \right] \tag{11}$$

3) Fusion: The fusion of above two representative vectors is designed as a propagation process with cross iterations. During each round of updating, their computational expressions are correlated with each other. The index number of updating rounds is denoted as q which ranges from 1 to Q.

In the q-th round, the $R_i^{(Co)}$ is updated through the following formula:

$$R_i^{(Co)(q+1)} = \sigma_2 \left[R_i^{(Co)(q)} + \frac{1}{|p|} \sum_{j=1}^{|p|} T_{ij}^{(q)} \right] \tag{12}$$

Algorithm 1 Encoding of Local Features

INPUT: u_i, p_j, γ, θ, m, n, q
OUTPUT: L_{ij}
for $i = 1 \rightarrow |u|$ **do**
  Represent social relation vector as Eq. (1)
  Transform A_s into $A_s^{(1)}$ as Eq. (2)
  for $\theta = 1 \rightarrow \eta$ **do**
    Transform $A_s^{(1)}$ into $A_s^{(2)}$ as Eq. (3) and Eq. (4)
  end for
  for $m = 1 \rightarrow M$ **do**
    for $n = 1 \rightarrow N$ **do**
      Compute $A_L^{(m)}$ as Eq. (5)
      Compute $R_i^{(Co)}$ as Eq. (6)
    end for
  end for
  for $j = 1 \rightarrow |p|$ **do**
    Compute $R_i^{(Se)}$ as Eq. (10) and Eq. (11)
    for $q = 1 \rightarrow Q$ **do**
      Update $R_i^{(Co)}$ as Eq. (12), Eq. (13) and Eq. (14)
      Update $R_i^{(Se)}$ as Eq. (15) and Eq. (16)
    end for
    Represent L_{ij} as Eq. (17)
  end for
end for

among, $\sigma_2(\cdot)$ is sigmoid activation function represented as:

$$\sigma_2(x) = \frac{1}{1 + \exp(-x)} \tag{13}$$

and $T_{ij}^{(q)}$ denotes transition matrix between user u_i and POI p_j, and is represented as:

$$T_{ij}^{(q)} = \sigma_1 \left[W_{L4} \cdot R_j^{(Se)(q)} + b_{L4} \right] \tag{14}$$

where W_{L4} is weight parameter and b_{L4} is bias parameter. Similarly, the $R_j^{(Se)}$ is updated through the following formula:

$$R_j^{(Se)(q+1)} = \sigma_2 \left[R_j^{(Se)(q)} + \frac{1}{|u|} \sum_{i=1}^{|u|} T_{ji}^{(q)} \right] \tag{15}$$

and $T_{ji}^{(q)}$ denotes transition matrix between POI p_j user u_i and , and is represented as:

$$T_{ji}^{(q)} = \sigma_1 \left[W_{L5} \cdot R_i^{(Co)(q)} + b_{L5} \right] \tag{16}$$

After Q rounds of iterations, the final representative vector is obtained as:

$$L_{ij} = \left[R_i^{(Co)(Q)} \oplus R_j^{(Se)(Q)} \right] \tag{17}$$

Pseudo code of this subsection is displayed in Algorithm 1.

C. Modeling of Global Features

In this research, global features mainly refer to latent relevance between users, and contain two aspects: static relevance and dynamic relevance. The CAE part is responsible for encoding the global features by considering two types of relevance. Fig. 4 illustrates main workflow of the CAE part, and utilizes two parts to demonstrate two types of relevance encoding. The former comes from static features such as personal profiles, and the latter derives from dynamic features like sequential POI records. They are respectively encoded into feature factors, and then concatenated into the final representative vector.

1) Static Relevance: As for user u_i, his profile generally contains multiple attributes which can be divided into structured types and unstructured types.

Structured attributes refer to those whose formats are one of several fixed options, e.g., sex, location. This type of data can be represented as vectorized formation via one-hot encoding mechanism. In one-hot encoding, only one bit is valid in a long coding sequence. It is a binary encoding rule in which the valid bit is denoted as 1. Unstructured attributes refer to those whose contents are not optional items, e.g., personal tags. This type of data can be further classified into numerical data and textual data. The former can be directly utilized for calculation, yet the latter needs to be encoded into vectorized forms. In particular, ten high-frequency words are selected as the word plate for counting. And the TF-IDF method is employed for such encoding procedure. A number of high-frequency words correspond to ten elements in the encoded vector. An element is set to 1 if corresponding word is involved, and 0 otherwise.

Encoding results of both types of attributes are integrated into a total vector. To unify value range, normalization processing is required to produce a vector $Q_i^{(st)}$. Supposing that $u_z\,(z = 1, 2, \cdots, |u|\,; z \neq i)$ denotes another different from user u_i, the static relevance between user u_i and user u_z is measured as:

$$F_3(u_i, u_z) = \sigma_1 \left[\alpha_{i,z}^{(st)} \cdot W_{G1} \cdot \left\| Q_i^{(st)} - Q_z^{(st)} \right\| + b_{G1} \right] \tag{18}$$

where W_{G1} is weight parameter, b_{G1} is bias parameter, and $a_{i,z}^{(st)}$ is the relevance weight between them which is defined as:

$$a_{i,z}^{(st)} = \begin{cases} \frac{\frac{\psi_s(i \cap z)}{\psi_s(z)}}{\sum_{f=1; f \neq i,z}^{|u|} \left[\frac{\psi_s(i \cap f)}{\psi_s(f)} \right]}, & i \neq z \\ 0, & i = z \end{cases} \tag{19}$$

where $u_f\,(f = 1, 2, , |u|\,; f \neq i, z)$ denotes another user different from u_i and u_z, $\psi_s(z)$ counts friends of user u_z, $\psi_s(f)$ counts friends of user u_f, $\psi_s(i \cap z)$ counts common friends between u_i and u_z, and $\psi_s(i \cap f)$ counts common friends between u_i and u_f. Thus, the static relevance vector between user u_i and user u_z is represented as:

$$R_{i,z}^{(st)} = \sigma_1 \left[W_{G2} \cdot F_3(u_i, u_z) + b_{G2} \right] \tag{20}$$

where W_{G2} is weight parameter, and b_{G2} is bias parameter.

2) Dynamic Relevance: Let $P_{i,\beta}\,(\beta = 1, 2, \cdots, Y)$ denote Y positions in location sequences of user u_i, where β is the index number. It is encoded into a more abstract feature vector:

$$\Phi_{i,\beta}^{(dy)} = \lambda_1 \cdot W_{G3} \cdot P_{i,\beta} + (1 - \lambda_1) \cdot W_{G4} \cdot P_{i,(\beta-1)} + b_{G3} \tag{21}$$

where λ_1 is the trade-off parameter, W_{G3} and W_{G4} are weight parameters, and b_{G3} is the bias parameter. For the first position,

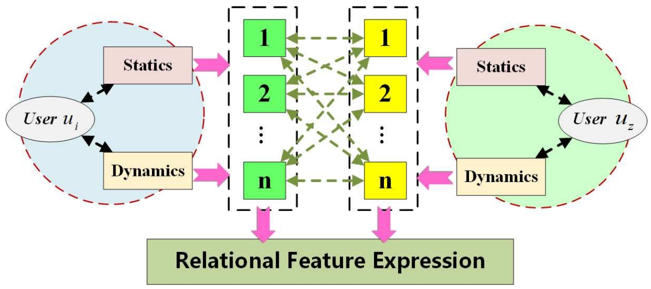

Fig. 4: Illustration of the CAE architecture.

the $P_{i,(\beta-1)}$ equals to 0. As the number of location records varies with different users, $\Phi_{i,\beta}^{(dy)}$ can be further computed as:

$$X_{i,\beta}^{(dy)} = \frac{1}{Y}\sum_{\beta=1}^{Y} \omega_\Omega \cdot \Phi_{i,\beta}^{(dy)} \tag{22}$$

where ω_Ω is the weight parameter corresponding to totally Y transformed position vectors of user u_i. The dynamic relevance between user u_i and user u_z is measured as:

$$F_4\left(u_i, u_z\right) = \sigma_1\left[\alpha_{i,z}^{(dy)} \cdot W_{G5} \cdot \left\|X_i^{(dy)} - X_z^{(dy)}\right\| + b_{G5}\right] \tag{23}$$

where W_{G5} is weight parameter, b_{G5} is bias parameter, and $\alpha_{i,z}^{(dy)}$ is the relevance weight between them which is defined as:

$$a_{i,z}^{(dy)} = \begin{cases} \frac{\frac{\psi_P(i\cap z)}{\psi_P(z)}}{\sum_{f=1;f\neq i,z}^{|u|}\left[\frac{\psi_P(i\cap f)}{\psi_P(f)}\right]}, & i \neq z \\ 0, & i = z \end{cases} \tag{24}$$

where $\psi_p\left(z\right)$ counts position records of user u_z, $\psi_p\left(f\right)$ counts position records of user u_f, $\psi_p\left(i\cap z\right)$ counts common positions between u_i and u_z, and $\psi_s\left(i\cap f\right)$ counts common positions between u_i and u_f. Thus, the dynamic relevance vector between user u_i and user u_z is represented as:

$$R_{i,z}^{(dy)} = \sigma_1\left[W_{G6} \cdot F_4\left(u_i, u_z\right) + b_{G6}\right] \tag{25}$$

where W_{G6} is weight parameter, and b_{G6} is bias parameter.

3) Integration: The integration of two representative vectors is to learn a total relevance matrix between user u_i and all the other users. And the integration process actually undergoes an iterative updating process. The index number of iterations is assumed as k and ranges from 1 to K.

Firstly, concatenation of two representative vectors leads to the initial state of iterations, which is denoted as:

$$R_{i,z}^{(0)} = R_{i,z}^{(st)} \oplus R_{i,z}^{(dy)} \tag{26}$$

In the k-th iterative round, forward hidden state $G_{i,z}^{(k)}$ is updated through the following operation:

$$G_{i,z}^{(k)} = W_{G7} \cdot R_{i,z}^{(k)} + T_{i,z} \cdot G_{i,z}^{(k-1)} + b_{G7} \tag{27}$$

where W_{G7} is weight parameter, b_{G7} is bias parameter, and $T_{i,z}$ is the transition matrix between u_i and u_z. As two users are the same type of entities, transition between them

Algorithm 2 Encoding of Global Features

INPUT: u_i, u_z, $P_{i,\beta}$, λ_1, λ_2 and k
OUTPUT: G_i

```
for i = 1 → |u| do
  for z = 1 → |u| and z ≠ i do
    Measure the static relevance between u_i and u_z as Eq. (18)
    Compute relevance weight of them as Eq. (19)
    Represent relevance factor as Eq. (20)
    for β = 1 → Y do
      Encode location sequence P_{i,β} as Eq. (21)
      Map Φ^{(dy)}_{i,β} as Eq. (22)
      Measure dynamic relevance between u_i and u_z as Eq. (23)
      Compute relevance weight of them as Eq. (24)
      Represent relevance factor as Eq. (25)
    end for
    Compute Initial status of relevance as Eq. (26)
    for k = 1 → K do
      Update forward hidden state as Eq. (27)
      Compute transition matrix as Eq. (28)
      Update R^{(k)}_{i,z} as Eq. (29)
    end for
    Specialize G^{(k)}_{i,z} as Eq. (30)
  end for
end for
```

is assumed as bi-directional. Thus the $T_{i,z}$ can be further expressed as the following formula:

$$T_{i,z} = \lambda_2 \cdot \sum_{z=1;z\neq i}^{|u|} T_{i\to z} + (1-\lambda_2) \cdot \sum_{i=1;i\neq z}^{|u|} T_{z\to i} \tag{28}$$

where λ_2 is the trade-off parameter. And $R_{i,z}^{(k)}$ is updated as follows:

$$R_{i,z}^{(k)} = W_{G8} \cdot R_{i,z}^{(k-1)} + b_{G8} \tag{29}$$

where W_{G8} is weight parameter, and b_{G8} is bias parameter.

After K rounds of iterations, the obtained $G_{i,z}^{(k)}$ denotes final relevance vector between u_i and u_z. Enumerating z of $G_{i,z}^{(k)}$ from 1 to $|u|$ leads to a static relevance matrix for user u_i, which is expressed as the following format:

$$G_i = \left\{\left[G_{i,1}^{(K)}\right]^T, \cdots, \left[G_{i,i-1}^{(K)}\right]^T, \left[G_{i,i+1}^{(K)}\right]^T, \cdots, \left[G_{i,|u|}^{(K)}\right]^T\right\} \tag{30}$$

D. Recommendation

Given above two factors L_{ij} and G_i, it is expected to generate interaction result between user u_i and POI p_j. Due to the fact that L_{ij} is the form of vector while G_i is the form of matrix, they need to be mapped into unified forms. Hence, two basic multi-layer perception (MLP) networks are introduced for this purpose:

$$Z_L\left(u_i, p_j\right) = \sigma_1\left[MLP_1\left(L_{ij}\right)\right] \tag{31}$$

$$Z_g\left(u_i\right) = \sigma_3\left[MLP_2\left(G_i\right)\right] \tag{32}$$

TABLE I: Statistics of experimental datasets

Attribute	*Foursquare*	*Gowalla*	*Brightkite*
# of users	3728	2516	2739
# of POIs	28979	43727	13068
# of check-ins	923742	764973	593481
# of social links	46581	31584	19642
Avg. sentence length	47	36	33

where their parameters can be learned during training, and σ_3 denotes the leaky ReLU activation function. The obtained $Z_L(u_i, p_j)$ and $Z_g(u_i)$ are two vectors with the same dimensions. The predicted interaction result between user u_i and POI p_j is calculated as:

$$\tilde{O}_{ij} = \sigma_2 \left\{ W_1 \cdot Z_L(u_i, p_j) \cdot [Z_g(u_i)]^T + b_1 \right\} \tag{33}$$

Note that the range of $\tilde{O}_{ij}$ is $(0, 1)$. The prediction of interaction results can be viewed as a binary classification problem. 0 refers to that no interaction result exists between them and 1 refers to the existence of interaction. Given this, learning goal of the Deep-PR can be summarized as searching for the minimum of the following formula:

$$B = \sum_{i=1}^{|u|} \sum_{j=1}^{|p|} \left\{ \lambda_3 \cdot \left\| \tilde{O}_{ij} - O_{ij} \right\|_F^2 + (1 - \lambda_3) \cdot \|\Theta\|_F^2 \right\} \tag{34}$$

where O_{ij} is the real interaction result between user u_i and POI p_j, $\|\cdot\|_F^2$ denotes the Frobenius norm, Θ denotes the set of parameters, and λ_3 is the trade-off parameter. Finally, the Adam optimizer [35] is set as the learning method to solve the above optimization problem. As for training of Deep-PR, all of the parameters inside the whole model are randomly assigned a value firstly. The Deep-PR can be regarded as a model that integrates HAE and CAE modules. And backward propagation-based training method is introduced here to update gradient factors inside forward process of Deep-PR. Through such process, the parameters inside HAE an CAE can be also learned.

IV. Experiments and Analysis

This section presents the detailed process for evaluating performance of the proposed Deep-PR on three real-world datasets of mobile social networks.

A. Datasets

The construction of experimental scenarios derives from three publicly available datasets that are commonly used for such purpose: Gowalla [36], Foursquare [37] and Brightkite [36]. Initial datasets as well as some preprocessing operations are described as follows:

Foursquare: Foursquare is a famous location-based mobile social application, and encourages mobile users to share their instantaneous locations with others via check-ins. The dataset contains data from January, 2011 to July, 2011, and was firstly collected by Gao et al. from another popular social website Twitter.

Gowalla: Gowalla was a location-centered social website which enables users to share their locations via publishing check-ins. The dataset was collected by Cho et al. with the assistance of Gowalla API. Its records last from February, 2009 to October, 2010.

Brightkite: Brightkite was once another location-based social service provider to make users publish check-ins everywhere. The dataset was also collected by Cho et al. utilizing official API. It contains records over the period from April, 2008 to October, 2010.

Data records of all the datasets contain users, positions, check-ins, and social relations among users. To reduce sparsity of initial datasets, users or positions possessing less than ten interaction records have been filtered out. To ensure relatively rich social information, users having less than six social links are removed from the datasets. For each dataset, each POI is a square block with 0.05 (longitude) $\times$ 0.05 (latitude). As for textual contents of POI, we crawl review and description information mainly from two sources: Yelp website [1] and Baidu Map [2]. All the texts associated with a POI are viewed as a sentence that can be semantically modeled. As all these datasets lack profiles of users, user profiles from another social platforms need to be leveraged for analog. To ensure fairness, user profiles are uniformly crawled from a Chinese social media named Sina Weibo and randomly populated into users of datasets. After preprocessing procedures, statistics of the final experimental datasets are listed in TABLE I.

B. Experimental Settings

Data of each dataset is divided into two parts: training set and testing set. The former is assumed as historical records and thus used for training models. The latter is viewed as real data happening in the future, and is adopted to testify efficiency of recommendation results. The POIs suggested to users are compared with POIs in testing set to measure effect of recommendation results. Obviously, a larger number of recommended POIs occurring in testing set indicate better recommendation effect. As for measurement, four typical metrics that are commonly used for evaluating POIs recommendations are selected here. They are $Precision@C$, $Recall@C$, and $NDCG@C$, where $x@C$ denotes the value of x when the number of POIs recommended to each user is C. And detailed descriptions are illustrated as follows:

Precision@C: It refers to ratio of correctly suggested POIs in all the recommended POIs. The metric is called Pr@C for short and computed as:

$$Pr@C = \frac{1}{|u|} \sum_{i=1}^{|u|} \frac{\psi[J_{rec}(u_i) \cap J_{test}(u_i)]}{\psi[J_{rec}(u_i)]} \tag{35}$$

where $J_{rec}(u_i)$ denotes the set of POIs recommended to user u_i, $J_{test}(u_i)$ denotes the set of POIs of user u_i occurring in testing set, and $\psi(\cdot)$ is the counting operation.

[1] http://www.yelp.com
[2] http://map.baidu.com

TABLE II: List of hyper-parameters that may influence algorithm running.

Parameters	Description	Setting
N	The number of filter cores	5
Q	The number of iterative rounds in HAE	5
K	The number of iterative rounds in CAE	5
λ_1	Tuning parameters to control weight of specific parts	0.5
λ_2	Tuning parameters to control weight of specific parts	0.5
λ_3	Tuning parameters to control weight of specific parts	0.6
batch size	The number of samples that will be input into model each time	16
epoch size	The number of samples that will be input into model each time	8
learning rate	The length of one stride during optimization processes	0.001

TABLE III: Precision and recall results on Foursquare dataset

Method	Precision results			Recall results		
	Pr@5	Pr@8	Pr@10	Re@5	Re@8	Re@10
GE-LR [40]	0.01791	0.01022	0.00873	0.0732	0.0803	0.0964
PSG-LSTM [41]	0.02847	0.02459	0.01668	0.0944	0.1078	0.1387
PSG-GRU [42]	0.02646	0.02312	0.01837	0.0905	0.0994	0.1215
PRBPL [38]	0.03145	0.02807	0.02439	0.1134	0.1256	0.1438
CPAM [39]	0.03312	0.03023	0.02506	0.1252	0.1394	0.1515
Deep-PR	0.04056	0.03361	0.02933	0.1476	0.1769	0.1986

TABLE IV: Precision and recall results on Gowalla dataset

Method	Precision results			Recall results		
	Pr@5	Pr@8	Pr@10	Re@5	Re@8	Re@10
GE-LR [40]	0.01493	0.01009	0.00755	0.0378	0.0459	0.0571
PSG-LSTM [41]	0.02251	0.01736	0.01352	0.0517	0.0688	0.0822
PSG-GRU [42]	0.02347	0.01851	0.01517	0.0754	0.0932	0.1018
PRBPL [38]	0.02910	0.02429	0.02086	0.0853	0.0979	0.1165
CPAM [39]	0.02853	0.02457	0.02148	0.0914	0.1037	0.1082
Deep-PR	0.03324	0.02932	0.02566	0.1063	0.1209	0.1357

Recall@C: It refers to ratio of correctly suggested POIs in all the POIs of testing set. The metric is called Re@C for short and computed as:

$$Re@C = \frac{1}{|u|}\sum_{i=1}^{|u|}\frac{\psi\left[J_{rec}\left(u_i\right)\cap J_{test}\left(u_i\right)\right]}{\psi\left[J_{test}\left(u_i\right)\right]} \tag{36}$$

F-score@C: It is an overall format of precision and recall. The metric is called Fs@C for short and computed as:

$$Fs@C = \frac{2\cdot Pr@C\cdot Re@C}{Pr@C + Re@C} \tag{37}$$

NDCG@C: It refers to normalized discounted cumulative gain (NDCG), and implies ranking effectiveness of Top-C results. The metric is computed as:

$$NDCG@C = \frac{1}{|u|}\sum_{i=1}^{|u|}\left[\frac{1}{\Delta\left(u_i\right)}\sum_{c=1}^{C}\frac{2^{\delta_i(c)}-1}{\log\left(c+1\right)}\right] \tag{38}$$

where c is the index number of all the C recommended POI, and $\delta_i\left(c\right)$ denotes the relation indicator between user u_i and the c-th POI suggested to him. In detail, $\delta_i\left(c\right)$ equals to 1 if the c-th POI is correctly recommended and 0 otherwise.

To verify the superiority of the proposed Deep-PR compared to general POI recommendation methods, some classical approaches for this purpose are selected as baselines. The Deep-PR and baselines are all implemented on four datasets to compare their performance with respect to above metrics.

TABLE V: Precision and recall results on Brightkite dataset

Method	Precision results			Recall results		
	Pr@5	Pr@8	Pr@10	Re@5	Re@8	Re@10
GE-LR [40]	0.01639	0.01266	0.01038	0.0385	0.0421	0.0564
PSG-LSTM [41]	0.02316	0.01856	0.01657	0.0474	0.0667	0.0683
PSG-GRU [42]	0.02209	0.01762	0.01529	0.0597	0.0703	0.0826
PRBPL [38]	0.02877	0.02394	0.02015	0.0782	0.0915	0.0997
CPAM [39]	0.02683	0.02326	0.01909	0.0928	0.1059	0.1141
Deep-PR	0.03185	0.02848	0.02653	0.1028	0.1148	0.1387

GE-LR: It models context-aware factors via bipartite graph theory. Then, graph-level features are embedded to establish a location recommendation method.

PSG-LSTM: It considers auxiliary factors from three aspects: user preferences, social influence and geographical comments. And they are fused into the long short-term memory model (LSTM) to realize POI recommendations.

PSG-GRU: Similar to PSG-LSTM, it integrates three aspects of factors into the gated recurrent unit model (GRU) for POI recommendations.

PRBPL: It jointly considers geographical distance and POI categorical distance so that pairwise user preferences can be obtained from the initial data.

CPAM: It uses skip-gram to model POI features and logistic matrix factorization to model user preferences.

Including the proposed Deep-PR, there are totally eight methods involved in the whole experiments. The seven selected baseline methods are mostly classical methods that are usually used for evaluating POI recommendation effect. The GE-LR contains GE and LR two parts, in which GE part is implemented according to reference [40] and LR part is specially implemented. For PSG-LSTM and PSG-GRU, the LSTM part and GRU part are implemented according to references [41] and [42], and the PSG part is specially implemented. For PRBPL and CPAM, their descriptions can be found in [38] and [39].

All the experiments are carried out in a deep learning working station with 32-core CPU, 256-GB RAM and a GPU (RTX-2080-Ti). The proposed Deep-PR is implemented with the assistance of TensorFlow [3]. TABLE II lists setting for main hyper-parameters that may influence running efficiency. In processing layer of CNN, the number of filter cores N in Eq. (5) is set to 5, and the number of updating rounds in HAE is set to 5. Tunning parameter λ_1 in Eq. (21) and λ_2 in Eq. (28) are set to 0.5, and λ_3 in Eq. (34) is set to 0.6. The number of iteration rounds in Eq. (30) is set to 5. For model implementation, not all the data is input into the model directly. Instead, it is input into the model via the batch-to-batch mode. The batch-size is set to 16, and the epoch number is set to 8. The learning rate in experiments is initially set to 0.001. As the Deep-PR is mainly tested in terms of different recommendation sizes, the whole experiments just have such one ratio between training data and testing data. In each experimental group, the experiment will not be implemented only once. Instead, a group will be conducted five times to obtain five results. The final result for a group equals to average value of the five results.

[3] http://tensorflow.google.cn/

C. Results and Analysis

The precision and recall results on three datasets are listed in TABLE III, TABLE IV and TABLE V, respectively. When the number of recommended POIs increases from 5 to 10, values of precision results tend to get smaller, while values of recall results tend to get larger. The obtained results on Foursquare dataset fluctuate volatilely, and those on Brightkite dataset fluctuate gently. Of all these approaches, the proposed Deep-PR always performs better than those of baselines. Even compared with two of proper baselines: PRBPL and CPAM, the proposed Deep-PR can still have an improvement of at least 10%. Two possible reasons can be deduced to explain above observations. For one thing, the Deep-PR considers both local and global feature factors, so that deep distributed learning realized to enhance feature expression. For another, the Deep-PR respectively updates two feature subspaces via two different multi-round iterations, so that deep representation of feature spaces is reoptimized. The collaborative effect of above reasons contributes to more precise recommendations.

The F-score results on three datasets are listed in Fig. 5 which contains three subfigures. Among, each subfigure has three clusters of values, corresponding to values of F-score@5, F-score@8 and F-score@10. Overall, the F-score results show descending tendency while the number of recommended POIs changing from 5 to 10. It can be clearly observed that three deep learning-based methods outperform others all the time, and the proposed Deep-PR is superior to the other two. The NDCG results on three datasets under different sizes of training data are demonstrated in Fig. 6, separately. It has three subfigures, in which X-axis denotes different sizes of recommended POIs and Y-axis denotes values of metric NDCG. Although baselines show diverse performance status under different setting of scenarios, performance curves of the proposed Deep-PR are always superior to other curves. Especially when the proportion of training data switches from

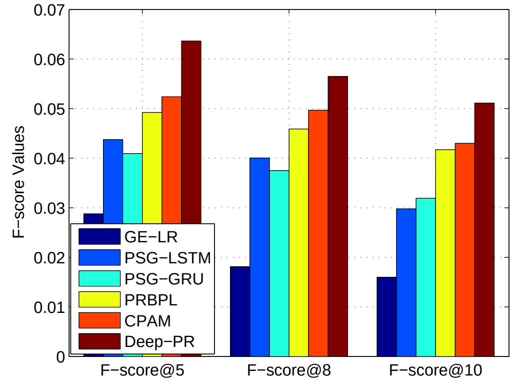

(a) Foursquare dataset

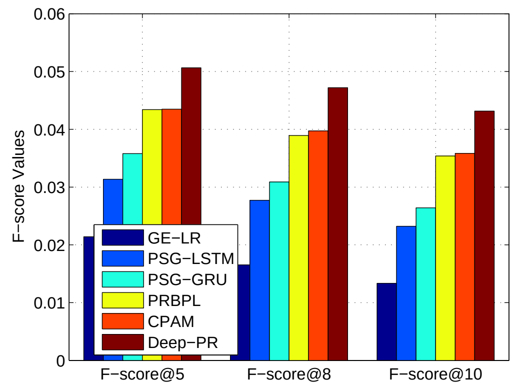

(b) Gowalla dataset

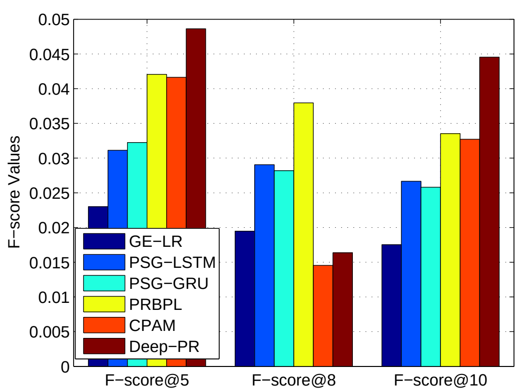

(c) Brightkite dataset

Fig. 5: F-score results on three datasets.

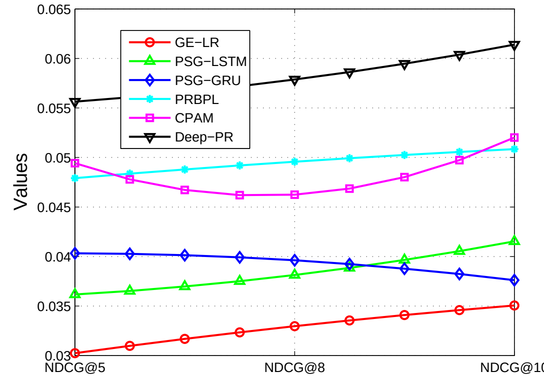

(a) Foursquare dataset

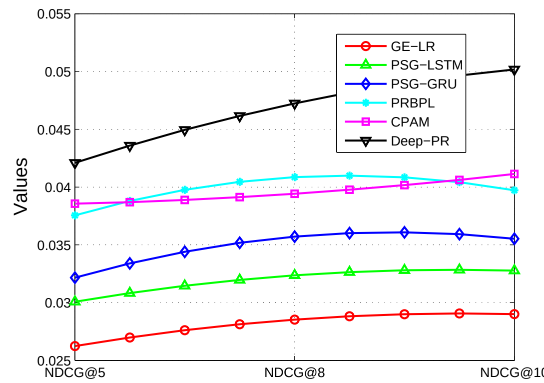

(b) Gowalla dataset

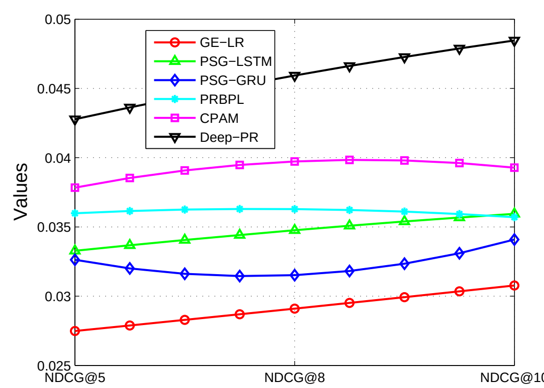

(c) Brightkite dataset

Fig. 6: NDCG results on three dataset.

50% to 60%, Deep-PR has no obvious performance promotion, because it has been trained to achieve a relatively stable status. Main reasons for obtainment of the results can be also attributed to two aspects. Firstly, deep representation and distributed learning not only extract more latent feature factors, but also improve robustness of model. Secondly, the introduction of propagation procedures further optimizes feature abstraction. The recursive effect of them makes the feature spaces more fine-grained.

Having evaluated efficiency of the proposed Deep-PR, another set of experiments are conducted to explore its stability by testing sensitivity to parameter change. In this group of experiments, just performance fluctuation of Deep-PR itself under different parameter settings is visualized, without comparing with baselines. In detail, performance tendency in terms of four metrics is analyzed with the changing of two groups of parameters: size of recommended results and proportion of training data. Concretely, proportion is set to four values:

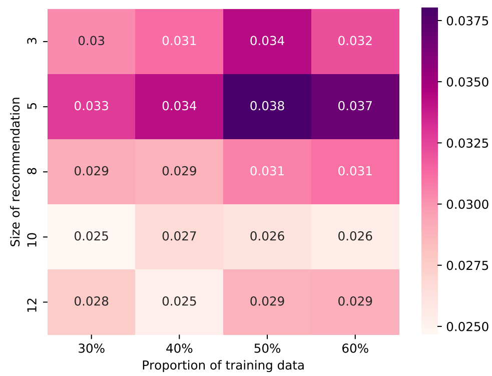

(a) Foursquare dataset

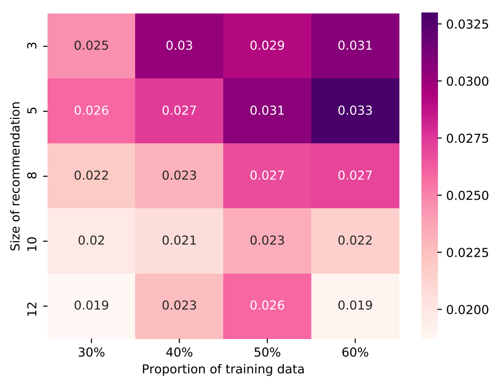

(b) Gowalla dataset

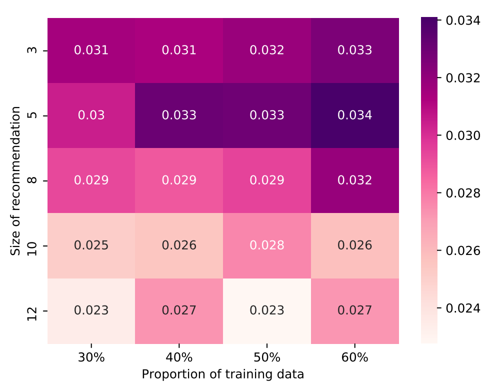

(c) Brightkite dataset

Fig. 7: Parameter sensitivity results of Deep-PR on three datasets in terms of precision.

(a) Foursquare dataset

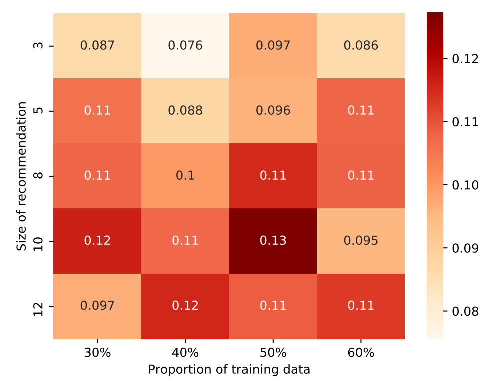

(b) Gowalla dataset

(c) Brightkite dataset

Fig. 8: Parameter sensitivity results of Deep-PR on three datasets in terms of recall.

30%, 40%, 50% and 60%, and size is set to give values: 3, 5, 8, 10 and12. Parameter sensitivity is assessed on three datasets with respect to above four evaluation metrics. And the results are illustrated in Fig. 7, Fig. 8, Fig. 9, and Fig. 10, corresponding to four metrics: precision, recall, F-score, and NDCG, separately. Each figure contains three subfigures, in which X-axis denotes different proportions of training data and Y-axis denotes different sizes of recommendation results. The smaller the chromaticity difference among blocks, the less the performance of the algorithm is affected by parameter change. When the size of recommendation increases, precision and F-score results show descending tendency, while recall and NDCG results show ascending tendency. Although values of metrics change with different scenario settings, the fluctuation is quite gentle. We analyze all the results and summarize three possible reasons for above phenomenon. Firstly, the whole feature space is modeled with considering both local and global factors, which is a comprehensive perspective

(a) Foursquare dataset

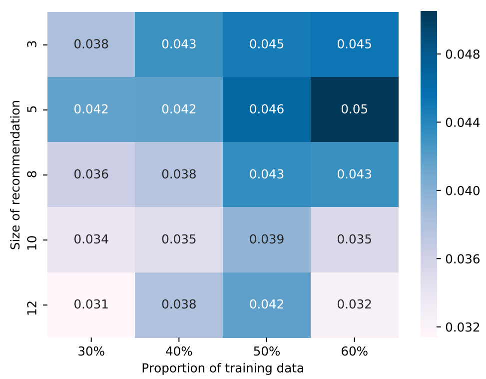

(b) Gowalla dataset

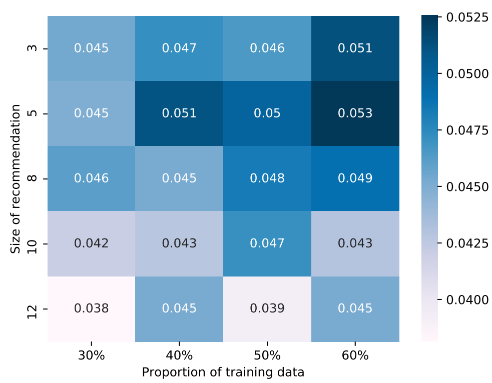

(c) Brightkite dataset

Fig. 9: Parameter sensitivity results of Deep-PR on three datasets in terms of F-score.

(a) Foursquare dataset

(b) Gowalla dataset

(c) Brightkite dataset

Fig. 10: Parameter sensitivity results of Deep-PR on three datasets in terms of NDCG.

to improve wideness of the feature space. Secondly, deep distributed learning is able to adaptively extract latent feature components, improving depth of the feature space. Thirdly, iterative computation operations are added to reconstruct feature space once more, so that fine-grained feature spaces can be obtained finally. Due to the three reasons, the proposed Deep-PR is not susceptible to parameter change.

D. Running Efficiency

To comprehensively assess performance of baseline methods and the proposed Deep-PR, the running speed is also discussed in this work. The experiments used 50% of data for training and 50% of data for testing, and the running time for training phase is tested. The average running speed results of experimental methods are listed in TABLE VI. For GE-LR, PSG-LSTM and PSG-GRU, they are involved in operations

TABLE VI: Main time complexity results of experimental methods.

Methods	Average running time (min)
GE-LR	17.7
PSG-LSTM	15.6
PSG-GRU	14.8
PRBPL	23.7
CPAM	20.6
Deep-PR	32.3

TABLE VII: PSBV values of experiments methods.

Methods	$\tau = 0.7$	$\tau = 0.65$	$\tau = 0.6$
GE-LR	0.3026	0.3424	0.3803
PSG-LSTM	0.4402	0.4769	0.5136
PSG-GRU	0.4625	0.5009	0.5393
PRBPL	0.3911	0.3983	0.4055
CPAM	0.4118	0.4301	0.4485
Deep-PR	0.2793	0.2593	0.2394

of deep neural networks and will cost more time than other baseline methods. The time length for each training round is about 17.7 minutes, 15.6 minutes and 14.8 minutes, separately. For PRBPL and CPAM, they are a bit more complicated than GE-LR, PSG-LSTM and PSG-GRU. Their time length values of training processes are 23.6 minutes and 20.6 minutes. As for the proposed Deep-PR, time length for a training round is about 32.3 minutes. There is no doubt that the proposed Deep-PR has no advantage in terms of running speed. In other words, the Deep-PR takes time cost as price to obtain better recommendation effect.

As the POI recommendation is a kind of time-sensitive application, running speed is a significant metric to evaluate the performance. To quantify the overall utility of the Deep-PR compared with others, an additional metric named as "Performance-Speed Balance Value (PSBV)" is further defined here for this purpose. The PSBV is preliminarily defined as follows:

$$PSBV = \tau \cdot \Delta_{performance} + (1 - \tau) \cdot \Delta_{speed} \tag{39}$$

where $\Delta_{performance}$ denotes utility value of performance, Δ_{speed} denotes utility value of running speed, and τ is the weight parameter for two parts. To ensure fairness, the $\Delta_{performance}$ and Δ_{speed} are both controlled into the range of $(0, 1)$. For a method, the $\Delta_{performance}$ equals to normalized value of its average F-score value. Naturally, higher average F-score values lead to higher $\Delta_{performance}$ values. While the Δ_{speed} equals to: one minus normalized value of its average running time. Naturally, higher average running time values lead to lower Δ_{speed} values. The τ denotes weight corresponding to performance, and the $(1 - \tau)$ denotes weight corresponding to running speed. When τ is set to 0.6, 0.65 and 0.7, the PSBV is listed in TABLE VII. It can be observed from the table that three methods with better performance cannot have higher PSBV values. Compared with PSG-LSTM and PSG-GRU, PSBV value of Deep-PR is about 30%-50% lower compared with them.

Frankly speaking, the deep information fusion can bring good performance to some extent, yet running speed still needs to be optimized in future works.

V. Conclusions and Future Works

MEN has been widely regarded as an indispensable part in future 5G communication networks. Correspondingly, providing recommendation service for MEN users is worth deep investigation. As simple user-location data are usually sparse and not informative, existing approaches attempted to extend feature spaces from contextual patterns and semantic patterns. Nevertheless, they mainly focused on internal features of users, yet ignoring potential external features among them. The combination of distributed learning and deep representative learning is a proper solution. To remedy such gaps, this paper proposes Deep-PR, a deep distributed learning-based POI recommendation. It separates the whole feature spaces into local part and global part. The modeling of the subspaces is implemented through a combination of deep representative learning and iterative computation. Their collaborative effect contributes to a feature space with stronger ability of feature expression. Finally, experiments on three real-world datasets show that the proposed Deep-PR outperforms baselines in terms of four metrics.

Certainly, this work assumes that social activities in different platforms are independent. But real-world social activities are always cross-platform, as many users register accounts in different platforms to acquire more fruitful experience. Thus, social activities that belong to different platforms are interactively correlated [43]. This point is still ignored by almost all of existing researches, regardless of ours and others. In fact, the model training inside a single platform can be viewed as a learning task. It is expected to train an integrated model oriented to hybrid social platforms through the joint learning of multiple tasks, so that generalization of recommendation can be well promoted. This is an important working direction of our research team in the future.

References

[1] Z. Guo and H. Wang, "A Deep Graph Neural Network-based Mechanism for Social Recommendations," *IEEE Trans. Ind. Informatics*, vol. 17, no. 4, pp. 2776-2783, 2021.

[2] Q. Zhang et al., "Graph Neural Networks-driven Traffic Forecasting for Connected Internet of Vehicles," *IEEE Trans. Netw. Sci. Eng.*, doi: 10.1109/TNSE.2021.3126830.

[3] D. Meng et al., "A Data-driven Intelligent Planning Model for UAVs Routing Networks in Mobile Internet of Things," *Comput. Commun.*, vol. 179, pp. 231-241, 2021.

[4] K. Yu et al., "Secure Artificial Intelligence of Things for Implicit Group Recommendations," in *IEEE Internet Things J.*, vol. 9, no. 4, pp. 2698-2707, 2022.

[5] C. Feng et al., "Blockchain-based Cross-domain Authentication for Intelligent 5G-enabled Internet of Drones," *IEEE Internet Things J.*, doi: 10.1109/JIOT.2021.3113321.

[6] H. -X. Hu, Z. -W. Jiang, Y. -F. Zhao, Y. Zhang, H. Wang and W. Wang, "Network Representation Learning-Enhanced Multisource Information Fusion Model for POI Recommendation in Smart City," *IEEE Internet Things J.*, vol. 8, no. 12, pp. 9539-9548, 2021.

[7] Y. Gong et al., "Nonlinear MIMO for Industrial Internet of Things in Cyber Physical Systems," *IEEE Trans. Ind. Informatics*, vol. 17, no. 8, pp. 5533-5541, 2021.

[8] D. Xu, P. Ren, J. A. Ritcey, "Independence-Checking Coding for OFDM Channel Training Authentication: Protocol Design, Security, Stability, and Tradeoff Analysis," *IEEE Trans. Inf. Forensics and Security*, vol. 14, no. 2, pp. 387-402, 2018.

[9] Z. Guo et al., "Graph embedding-based intelligent industrial decision for complex sewage treatment processes," *Int. J. Intell. Syst.*, doi: 10.1002/int.22540.

[10] Z. Zhou et al., "Spatio-Temporal Feature Encoding for Traffic Accident Detection in VANET Environment," *IEEE Trans. Intell. Transpor. Syst.*, 2022, early access, doi: 10.1109/TITS.2022.3147826.

[11] L. Tan et al., "Speech Emotion Recognition Enhanced Traffic Efficiency Solution for Autonomous Vehicles in a 5G-Enabled Space-Air-Ground Integrated Intelligent Transportation System," *IEEE Trans. Intell. Transpor. Syst.*, 2021, early access, doi: 10.1109/TITS.2021.3119921.

[12] F. Ding et al. "Perceptual Enhancement for Autonomous Vehicles: Restoring Visually Degraded Images for Context Prediction via Adversarial Training," *IEEE Trans. Intell. Transpor. Syst.*, 2021, early access, doi: 10.1109/TITS.2021.3120075.

[13] Z. Wang et al., "Towards Privacy-preserving Incentive for Mobile Crowdsensing Under An Untrusted Platform," in *Proc. of 2019 IEEE Conference on Computer Communications*, Paris, France, 2019, pp. 2053-2061.

[14] L. Huang et al, "Multi-modal Bayesian embedding for point-of-interest recommendation on location-based cyber-physical-social networks," *Future Gener. Comput. Syst.*, vol. 108, pp. 1119-1128, 2020.

[15] X. Xiong et al., "Where to go: An effective point-of-interest recommendation framework for heterogeneous social networks," *Neurocomputing*, vol. 373, pp. 56-69, 2020.

[16] W. Wang et al., "Geography-Aware Inductive Matrix Completion for Personalized Point-of-Interest Recommendation in Smart Cities," *IEEE Internet Things J.*, vol. 7, no. 5, pp. 4361-4370, 2020.

[17] W. Wang et al., "Trust-Enhanced Collaborative Filtering for Personalized Point of Interests Recommendation," *IEEE Trans. Ind. Informatics*, vol. 16, no. 9, pp. 6124-6132, 2020.

[18] Y. Lyu et al., "iMCRec: A multi-criteria framework for personalized point-of-interest recommendations," *Inf. Sci.*, vol. 483, pp. 294-312, 2019.

[19] Y. Si, F. Zhang, W. Liu, "An adaptive point-of-interest recommendation method for location-based social networks based on user activity and spatial features," *Knowl. Based Syst.*, vol. 163, pp. 267-282, 2019.

[20] R. Li, Y. Shen, Y. Zhu, "Next Point-of-Interest Recommendation with Temporal and Multi-level Context Attention," in *Proc. of 2018 IEEE International Conference on Data Mining, Singapore*, 2018, pp. 1110-1115.

[21] J. Yin et al., "ADPR: An Attention-based Deep Learning Point-of-Interest Recommendation Framework," in *Proc. of 2019 International Joint Conference on Neural Networks*, Budapest, Hungary, 2019, pp. 1-8.

[22] X. Jiao et al., "A novel next new point-of-interest recommendation system based on simulated user travel decision-making process," *Future Gener. Comput. Syst.*, vol. 100, pp. 982-993, 2019.

[23] Z. Zhang et al., "VCG: Exploiting visual contents and geographical influence for Point-of-Interest recommendation," *Neurocomputing*, vol. 357, pp. 53-65, 2019.

[24] S. Liu, L. Wang, "A self-adaptive point-of-interest recommendation algorithm based on a multi-order Markov model," *Future Gener. Comput. Syst.*, vol. 89, pp. 506-514, 2018.

[25] X. Zhou, C. Mascolo, Z. Zhao, "Topic-Enhanced Memory Networks for Personalised Point-of-Interest Recommendation," in *Proc. of the 25th ACM SIGKDD International Conference on Knowledge Descovery & Data Mining*, Anchorage, AK, USA, 2019, pp. 3018-3028.

[26] B. Chang et al., "Content-Aware Successive Point-of-Interest Recommendation," in *Proc. of the 2020 SIAM International Conference on Data Mining*, Cincinnati, Ohio, USA, 2020, pp. 100-108.

[27] B. Chang et al., "Content-Aware Hierarchical Point-of-Interest Embedding Model for Successive POI Recommendation," in *Proc. of the Twenty-Seventh International Joint Conference on Artificial Intelligence*, Stockholm, Sweden, 2018, pp. 3301-3307.

[28] B. Lin et al., "CARec: Content-Aware Point-of-Interest Recommendation via Adaptive Bayesian Personalized Ranking," *Aust. J. Intell. Inf. Process. Syst.*, vol. 15, no. 3, pp. 61-68, 2019.

[29] S. Xing et al., "Content-Aware Point-of-interest Recommendation Based on Convolutional Neural Network," *Appl. Intell.*, vol. 49, no. 3, pp. 858-871, 2019.

[30] L. Zhu et al., "SEM-PPA: A semantical pattern and preference-aware service mining method for personalized point of interest recommendation," *J. Netw. Comput. Appl.*, vol. 82, pp. 35-46, 2017.

[31] S. Jiang et al., "Author Topic Model-Based Collaborative Filtering for Personalized POI Recommendations," *IEEE Trans. Multimedia*, vol. 17, no. 6, pp. 907-918, 2015.

[32] J. He, X. Li, L. Liao, "Category-aware Next Point-of-Interest Recommendation via Listwise Bayesian Personalized Ranking," in *Proc. of the Twenty-Sixth International Joint Conference on Artificial Intelligence*, Melbourne, VIC, Australia, 2017, pp. 1837-1843.

[33] M. Aliannejadi, D. Rafailidis, F. Crestani, "A Joint Two-Phase Time-Sensitive Regularized Collaborative Ranking Model for Point of Interest Recommendation," *IEEE Trans. Knowl. Data Eng.*, vol. 32, no. 6, pp. 1050-1063, 2020.

[34] B. Hu, M. Ester, "Social Topic Modeling for Point-of-Interest Recommendation in Location-Based Social Networks," in *Proc. of 2014 IEEE International Conference on Data Mining*, Shenzhen, China, 2014, pp. 845-850.

[35] S. Bock, M. Weiβ, "A Proof of Local Convergence for the Adam Optimizer," in *Proc. of 2019 International Joint Conference on Neural Networks*, Budapest, Hungary, 2019, pp. 1-8.

[36] E. Cho, S. A. Myers, J. Leskovec, "Friendship and mobility: user movement in location-based social networks," in *Proc. of the 17th ACM SIGKDD International Conference on Knowledge Discovery and Data Mining*, San Diego, CA, USA, 2011, pp. 1082-1090.

[37] H. Gao, J. Tang, H. Liu, "gSCorr: modeling geo-social correlations for new check-ins on location-based social networks," in *Proc. of the 21st ACM International Conference on Information and Knowledge Management*, Maui, HI, USA, 2012, pp. 1582-1586.

[38] Q. Liu, L. Mu, V. Sugumaran, C. Wang, and D. Han, "Pair-wise ranking based preference learning for points-of-interest recommendation," *Knowl. Based Syst.*, vol. 225, Article No. 107069, 2021.

[39] D. Yu, W. Wanyan, and D. Wang, "Leveraging contextual influence and user preferences for point-of-interest recommendation," *Multim. Tools Appl.*, vol. 80, no. 1, pp. 1487-1501, 2021.

[40] M. Xie et al., "Learning Graph-based POI Embedding for Location-based Recommendation," in *Proc. of the 25th ACM International Conference on Information and Knowledge Management*, New York, NY, USA, 2016, pp. 15-24.

[41] L. Huang, Y. Ma, S. Wang and Y. Liu, "An Attention-Based Spatiotemporal LSTM Network for Next POI Recommendation," *IEEE Trans. Serv. Comput.*, vol. 14, no. 6, pp. 1585-1597, 2021.

[42] H. Tan, D. Yao, T. Huang, B. Wang, Q. Jing and J. Bi, "Meta-Learning Enhanced Neural ODE for Citywide Next POI Recommendation," in *Proc.* of 2021 22nd IEEE International Conference on Mobile Data Management (MDM), Toronto, ON, Canada, 2021, pp. 89-98, doi: 10.1109/MDM52706.2021.00023.

[43] Z. Guo, K. Yu, Y. Li, G. Srivastava and J. C. -W. Lin, "Deep Learning-Embedded Social Internet of Things for Ambiguity-Aware Social Recommendations," *IEEE Trans. Netw. Sci. Eng.*, doi: 10.1109/TNSE.2021.3049262.

Zhiwei Guo (Member, IEEE) received a B.E. in Communications Engineering from Zhengzhou University, Zhengzhou, China, in 2013, and a Ph.D. in Communications and Information Systems from Chongqing University, Chongqing, China, in 2018. He was a lecturer at Chongqing Technology and Business University, China, from 2018 to 2020. Since 2021, he has been working as an Associate Professor at Chongqing Technology and Business University, Chongqing, China.

Dr. Guo is leading multiple national research projects in China, including with the National Natural Science Foundation of China, the Research Program of the National Language Commission of China, and the Humanities and Social Sciences Research Project of the Ministry of Education. He has authored more than 30 publications, including papers in prestigious journals/conferences such as IEEE Transactions on Industrial Informatics, IEEE Internet of Things Journal, IEEE Transactions on Fuzzy Systems, IEEE Transactions on Network Science and Engineering, IEEE Wireless Communications, IEEE Network, Future Generation Computer Systems, International Journal of Intelligent Systems, Neural Computing and Applications, Electronics Letters, Multimedia Tools with Applications, Computer Communications, and IEEE GLOBECOM. He serves as an editorial board member for the Journal of Information Security.

In 2017, he gave an oral presentation at the International Joint Conference on Artificial Intelligence (IJCAI 2017). His research interests focus on data mining and pattern recognition.

Keping Yu received the M.E. and Ph.D. degrees from the Graduate School of Global Information and Telecommunication Studies, Waseda University, Tokyo, Japan, in 2012 and 2016, respectively. He was a Research Associate, Junior Researcher, Researcher with the Global Information and Telecommunication Institute, Waseda University, from 2015 to 2019, 2019 to 2020, 2020 to 2022, respectively. He is currently an associate professor at Hosei University, Japan, a visiting scientist at the RIKEN Center for Advanced Intelligence Project, Japan, and a visiting professor at Bengbu University, China.

Dr. Yu has hosted and participated in more than ten projects, is involved in many standardization activities organized by ITU-T and ICNRG of IRTF, and has contributed to ITU-T Standards Y.3071 and Supplement 35. He received the IEEE Outstanding Leadership Award from IEEE BigDataSE 2021, the Best Paper Award from IEEE Consumer Electronics Magazine Award 2022 (1st Place Winner), IEEE ICFTIC 2021, ITU Kaleidoscope 2020, the Student Presentation Award from JSST 2014. He has authored more than 200 peer-review research papers and books, including over 55 IEEE/ACM Transactions papers. He is an Associate Editor of IEEE Open Journal of Vehicular Technology, Journal of Intelligent Manufacturing, Journal of Circuits, Systems and Computers. He has been a Guest Editor for more than 20 journals such as IEEE Transactions on Computational Social Systems, IEEE Journal of Biomedical and Health Informatics, and Renewable & Sustainable Energy Reviews. He served as general co-chair and publicity co-chair of the IEEE VTC2020-Spring 1st EBTSRA workshop, general co-chair of IEEE ICCC2020 2nd EBTSRA workshop, general co-chair of IEEE TrustCom2021 3nd EBTSRA workshop, session chair of IEEE ICCC2020, ITU Kaleidoscope 2016. His research interests include smart grids, information-centric networking, the Internet of Things, artificial intelligence, blockchain, and information security.

Neeraj Kumar (Senior Member, IEEE) received the Ph.D. degree in computer science engineering from Shri Mata Vaishno Devi University, Katra, India, in 2009.

He was a Postdoctoral Research Fellow with Coventry University, Coventry, U.K. He is currently an Associate Professor with the Department of Computer Science and Engineering, Thapar University, Patiala, India. He is a Visiting Professor with Coventry University. He has authored or coauthored more than 300 technical research papers in leading journals and conferences from IEEE, Elsevier, Springer, Wiley, and others. Some of his research findings are published in top-cited journals such as the IEEE TRANSACTIONS ON INDUSTRIAL ELECTRONICS, the IEEE TRANSACTIONS ON DEPENDABLE AND SECURE COMPUTING, the IEEE TRANSACTIONS ON INTELLIGENT TRANSPORTATION SYSTEMS, the IEEE TRANSACTIONS ON CLOUD COMPUTING, the IEEE TRANSACTIONS ON KNOWLEDGE AND DATA ENGINEERING, the IEEE TRANSACTIONS ON VEHICULAR TECHNOLOGY, the IEEE TRANSACTIONS ON CONSUMER ELECTRONICS, the IEEE NETWORK, the IEEE TRANSACTIONS ON COMMUNICATIONS, the IEEE TRANSACTIONS ON WIRELESS COMMUNICATIONS, the IEEE INTERNET OF THINGS JOURNAL, the IEEE SYSTEMS JOURNAL, the Future Generation Computer Systems, the Journal of Network and Computer Applications, and the Computer Communications. He has guided many Ph.D. and M.E./M.Tech. students. His research was supported by fundings from Tata Consultancy Service, the Council of Scientific and Industrial Research, and the Department of Science and Technology. He is leading the research group "Sustainable Practices for Internet of Energy and Security," where group members are working on the latest cutting-edge technologies.

Dr. Kumar was the recipient of the Best Research Paper awards from the 2018 IEEE International Conference on Communications and the IEEE Systems Journal in 2018. He is a Technical Program Committee Member and Reviewer of many international conferences across the globe. He is on the editorial board of the Journal of Network and Computer Applications, the IEEE COMMUNICATION MAGAZINE, the International Journal of Communication Systems, and Security and Privacy.

Wei Wei received his Ph.D. and M.S. degrees from Xi'an Jiaotong University in 2011 and 2005, respectively. Currently, he is a lecturer of Computer Science at Xi'an University of Technology. His research interests include computational electromagnetics, wireless sensor networks application, mobile computing, distributed computing, and pervasive computing.

Shahid Mumtaz received the master's degree in electrical and electronic engineering from the Blekinge Institute of Technology, Sweden, in 2006, and the Ph.D. degree in electrical and electronic engineering from the University of Aveiro, Portugal, in 2011. He has more than 12 years of wireless industry/academic experience. He has been with the Instituto de Telecomunicações since 2011, where he currently holds the position of Auxiliary Researcher and adjunct positions with several universities across the Europe–Asian Region. He is also a Visiting Researcher at Nokia Bell Labs. He is the author of four technical books, 12 book chapters, and over 150 technical papers in the area of mobile communications. He is an ACM Distinguished Speaker, the EiC of IET Quantum Communication, the Vice Chair of Europe/Africa Region-IEEE ComSoc: Green Communications and Computing Society, and the Vice-Chair of IEEE standard on P1932.1: Standard for Licensed/Unlicensed Spectrum Interoperability in Wireless Mobile Networks.

Mohsen Guizani (Fellow, IEEE) received B.S. (with distinction) and M.S. degrees in electrical engineering and M.S. and Ph.D. degrees in computer engineering from Syracuse University, Syracuse, NY, USA, in 1984, 1986, 1987, and 1990, respectively. He is currently a Professor in the Computer Science and Engineering Department, Qatar University, Qatar. Previously, he served in various academic and administrative positions at the University of Idaho, Western Michigan University, the University of West Florida, the University of Missouri-Kansas City, the University of Colorado-Boulder, and Syracuse University. His research interests include wireless communications and mobile computing, computer networks, mobile cloud computing, security, and smart grids. He is currently the Editor-in-Chief of the IEEE Network Magazine, serves on the editorial boards of several international technical journals and is the Founder and Editor-in-Chief of the Wireless Communications and Mobile Computing journal (Wiley). He is the author of nine books and more than 600 publications in refereed journals and conferences. He guest edited various special issues in IEEE journals and magazines. He also served as a member, chair, and general chair for various international conferences. Throughout his career, he received three teaching awards and four research awards. He is the recipient of the 2017 IEEE Communications Society Wireless Technical Committee (WTC) Recognition Award, the 2018 AdHoc Technical Committee Recognition Award for his contributions to outstanding research in wireless communications and ad-hoc sensor networks and the 2019 IEEE Communications and Information Security Technical Recognition (CISTC) Award for outstanding contributions to the technological advancement of security. He was the Chair of the IEEE Communications Society Wireless Technical Committee and the Chair of the TAOS Technical Committee. He served as the IEEE Computer Society Distinguished Speaker and is currently the IEEE ComSoc Distinguished Lecturer. He is a Senior Member of ACM.